CHEMISTRY OF MATERIALS

Article

pubs.acs.org/cm

"Guanigma": The Revised Structure of Biogenic Anhydrous Guanine

Anna Hirsch,[†] Dvir Gur,[‡] Iryna Polishchuk,[§] Davide Levy,[§] Boaz Pokroy,[§] Aurora J. Cruz-Cabeza,[∥] Lia Addadi,*[,‡] Leeor Kronik,*[,†] and Leslie Leiserowitz*[,†]

[†]Department of Materials and Interfaces, and [‡]Department of Structural Biology, Weizmann Institute of Science, Rehovoth 76100, Israel

[§]Department of Materials Science and Engineering, Technion, Haifa 3200003, Israel

[∥]School of Chemical Engineering and Analytical Sciences, University of Manchester, The Mill, Sackville Street, Manchester M13 9PL, United Kingdom

Supporting Information

ABSTRACT: Living organisms display a spectrum of wondrous colors, which can be produced by pigmentation, structural coloration, or a combination of the two. A relatively well-studied system, which produces colors via an array of alternating anhydrous guanine crystals and cytoplasm, is responsible for the metallic luster of many fish. The structure of biogenic anhydrous guanine was so far believed to be the same as that of the synthetic one, a monoclinic polymorph (denoted as α). Here we re-examine the structure of biogenic guanine, using detailed experimental X-ray and electron diffraction data, exposing troublesome inconsistencies, namely, a "guanigma". To address this, we sought alternative candidate polymorphs using symmetry and packing considerations and then utilized first-principles calculations to determine whether the selected candidates could be energetically stable. We identified theoretically a different monoclinic polymorph (denoted as β), were able to synthesize it, and confirmed using X-ray diffraction that it is this polymorph that occurs in biogenic samples. However, the electron diffraction data were still not consistent with this polymorph but rather with a theoretically generated orthorhombic polymorph (denoted as γ). This apparent inconsistency was resolved by showing how the electron diffraction pattern could be affected by crystal structural faults composed of offset molecular layers.

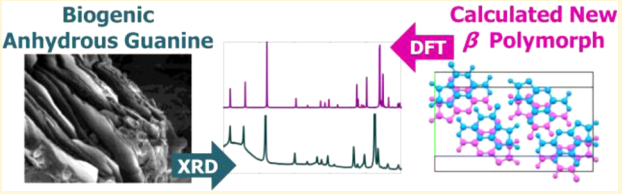

INTRODUCTION

Some of the most brilliant colors in nature are produced by the interaction of light with structured materials, which results in causing specific patterns of light scattering or reflection. Use of such structures, alone or through interaction with pigmentation, is widespread in the animal kingdom and can be found, for example, in birds,[1] fish,[2−4] reptiles,[5−7] and arthropods.[8,9] The colors are used for a variety of functions, including communication, mate recognition, camouflage, and vision enhancement.[10] The material of choice in many of these systems is guanine.

The metallic luster in fish scales results from constructive interference of visible light from multilayer arrays of guanine crystals separated by cytoplasm.[3,4] In certain spiders the guanine-based crystals produce a matte-white effect via scattering from small cuboidal crystals, while in others, stacks of guanine crystals in the form of thin plates generate a highly reflective silver color.[8,11] The widespread use of guanine crystals is probably due to its exceptionally high refractive index, n = 1.83 (in one direction), and to the fact that guanine is readily available in the cells as a nitrogenous metabolite.[8,12]

Recently there has been an increasing interest in rationalizing the optical properties of a variety of natural guanine-based optical systems[7,9,13−16] and in trying to mimic such systems for novel artificial devices.[17−20] The characteristic properties of these natural optical systems clearly depend on features of the crystal structure of guanine, and therefore it is imperative to have a comprehensive understanding of the guanine crystal structure.

The biogenic crystal structure of fish and spider guanine was found to be anhydrous.[21−23] The structure of the synthetic crystal of anhydrous guanine, at a temperature of 120 K, was found to be of monoclinic symmetry.[24] Previous studies by some of us suggested that the crystal structure of biogenic anhydrous guanine, extracted from fish[2] and spiders,[8] is identical to that of the published structure. However, already at that time some inconsistencies were noted that could not be easily explained. In the following we re-examine the experimental X-ray and electron diffraction patterns of the biogenic crystals from fish scales, spider integument, and synthetic crystals obtained from a dimethyl sulfoxide (DMSO) solution. The re-examination suggests that it is impossible to conclude unambiguously that the biogenic crystals possess the published monoclinic structure.

First, the information from the measured X-ray powder diffraction (XRPD) pattern of biogenic guanine platelet crystals

Received: September 11, 2015
Revised: November 4, 2015
Published: November 6, 2015

DOI: 10.1021/acs.chemmater.5b03549
Chem. Mater. 2015, 27, 8289−8297

was limited by preferred orientation. As a result, only strong reflections, corresponding to diffraction from the crystal plates, appeared in the diffraction pattern. However, the crystals were ideal for transmission electron microscopy (TEM) measurements, being only ~30 nm[25] thick (Figure 1A). We could not,

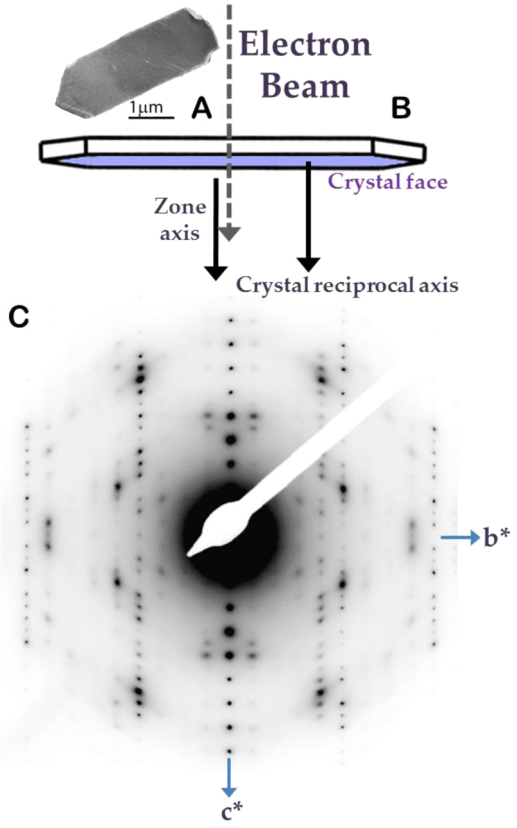

Figure 1. (A) TEM image of a fish plate-shaped crystal of anhydrous guanine. (B) Schematic representation of the guanine platelet in the TEM setup, in which the electron beam is perpendicular to the plate face and parallel to the proposed crystal zone axis. Thus, the proposed zone axis must be parallel to the crystal reciprocal axis normal to the crystal face. (C) Observed ED pattern of fish guanine. The reflection spots display *mm* Laue symmetry.

however, reconcile the measured electron diffraction (ED) pattern of the fish scale guanine with the published crystal structure of synthetic guanine. The dense array of distinct electron reflections (Figure 1C) displays *mm* Laue symmetry and is consistent with a crystal zone axis parallel to the electron beam, which is perpendicular to the plate face of the crystal. Thus, the proposed zone axis must be parallel to the crystal reciprocal axis normal to the crystal face (Figure 1B).[26] This evidence suggests prima facie that the fish guanine crystals appear in an orthorhombic arrangement. We, however, could not conclude whether the side faces delineated by the crystals (Figure 1A) form a zone axis perpendicular to the crystal plate, which would be a signature of an orthorhombic lattice. What, then, is the structure of the biogenic forms of fish and spider guanine?

The standard starting point in crystal structure determination is the solution of an unknown single crystal X-ray diffraction (XRD) pattern. This practice is difficult here, because the biogenic crystals available are too small to be used for single crystal XRD data collection even with intense synchrotron radiation. We therefore tackled this structure determination challenge by an unusual, comprehensive approach: First, we generated in silico a variety of polymorphic arrangements[27−31] of anhydrous guanine in monoclinic and orthorhombic structures, employing principles of symmetry and molecular packing considerations to guide us. We then utilized first-principles calculations to determine which of the generated polymorphs would be energetically stable. Specifically, we used state-of-the-art density functional theory (DFT) calculations with pairwise dispersive corrections[32] to address the structure and energetics of the guanine molecular crystals. We then computed the XRPD and ED patterns of the most favorable generated structures for a comparison with the experimental results. The lattice parameters obtained theoretically were then additionally refined against new high-resolution experimental XRPD data using the Rietveld method.[34] This allowed us to derive the polymorphic structures of biogenic fish and spider guanine and to glean information on possible fault structures in these crystals. We present, then, a multidisciplinary study involving various experimental and computational approaches to resolve the enigma of the structure of biogenic guanine; the "guanigma".

GENERATION OF POLYMORPHIC STRUCTURES

The published monoclinic crystal structure of anhydrous guanine[24] is composed of H-bonded layers, stacked along a 3.55 Å translational axis (Figure 2). As a starting point for the generation of guanine polymorphs, we transformed the (a', b', c') unit cell of the published structure into a new (a, b, c) unit cell, such that the H-bonded layer lies parallel to the bc plane (Figure 2B). The transformation yields unit cell parameters of a = 3.55 Å, b = 9.69 Å, c = 18.46 Å, and β = 118.3°. For convenience we shall refer to this structure as the α-polymorph. All the N−H···O, N−H···N, and even the C−H···N bonds are satisfied in the layer structure (Figure 2A). Thus, we can assume that reasonable polymorphic structures of anhydrous guanine will incorporate this layer motif. We note that based on pole-figure measurements made by Levy-Lior et al.,[2] the platelet face of the biogenic fish guanine crystals is parallel to the H-bonding layer.

The H-bonded system in the α-form is achieved in space group $P12_1/c1$ via a center of inversion ($\bar{1}$) and a 2-fold-screw axis (2_1) along the b-direction, where the combination of these two symmetry elements generates a glide plane perpendicular to b with a translation component along the c-axis (Figure 3A_1). Because the H-bonded layer motif is almost planar, it would remain the same on interchanging the 2-fold screw (along b) and the glide symmetry (along c) elements, to yield the H-bonded layer in space group $P112_1/b$ (Figure 3B_1). In this hypothetical crystal structure, which we label the β-polymorph, alternate H-bonded layers are related by translation along the a-axis, as in the α-polymorph, but the offset between neighboring layers is along the b-axis instead of along the c-axis (Figure 3A_2, B_2). It is noteworthy that the crystal structure of guanine monohydrate[35] reveals a stacking offset similar to the proposed β-form.

The possible formation of an orthorhombic γ-polymorph of fish guanine was proposed based on the preliminary analysis (vide supra) of the published ($0kl$) ED pattern, reported by Levy-Lior et al.[2] The lengths of the b^* and c^* reciprocal axes (0.1064, 0.0565 $Å^{-1}$) in this pattern correspond to $d(010)$ and $d(001)$ spacings of 9.4 and 17.7 Å, respectively. These values are sufficiently similar in length to those of the unit cell axes of the H-bonded layer of the α-form of guanine (9.69 and 18.46

DOI: 10.1021/acs.chemmater.5b03549
Chem. Mater. 2015, 27, 8289−8297

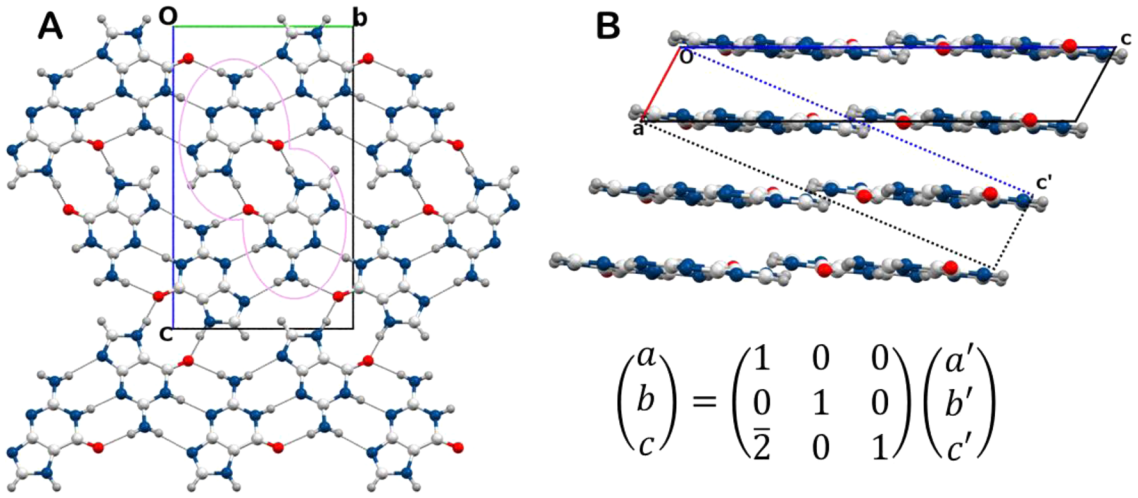

Figure 2. Crystal structure of the α-polymorph of anhydrous guanine: (A) The H-bonding (thin gray lines) motif in the crystal structure, viewed perpendicular to the molecular layer. The purple contour indicates a cyclic H-bonded dimer. (B) An edge-on view, along the *b*-axis, of the stacked layer of H-bonded molecules, together with the transformation matrix that relates the original (dashed lines) and transformed (solid lines) unit cell. After the transformation the molecules lie in the *bc* plane.

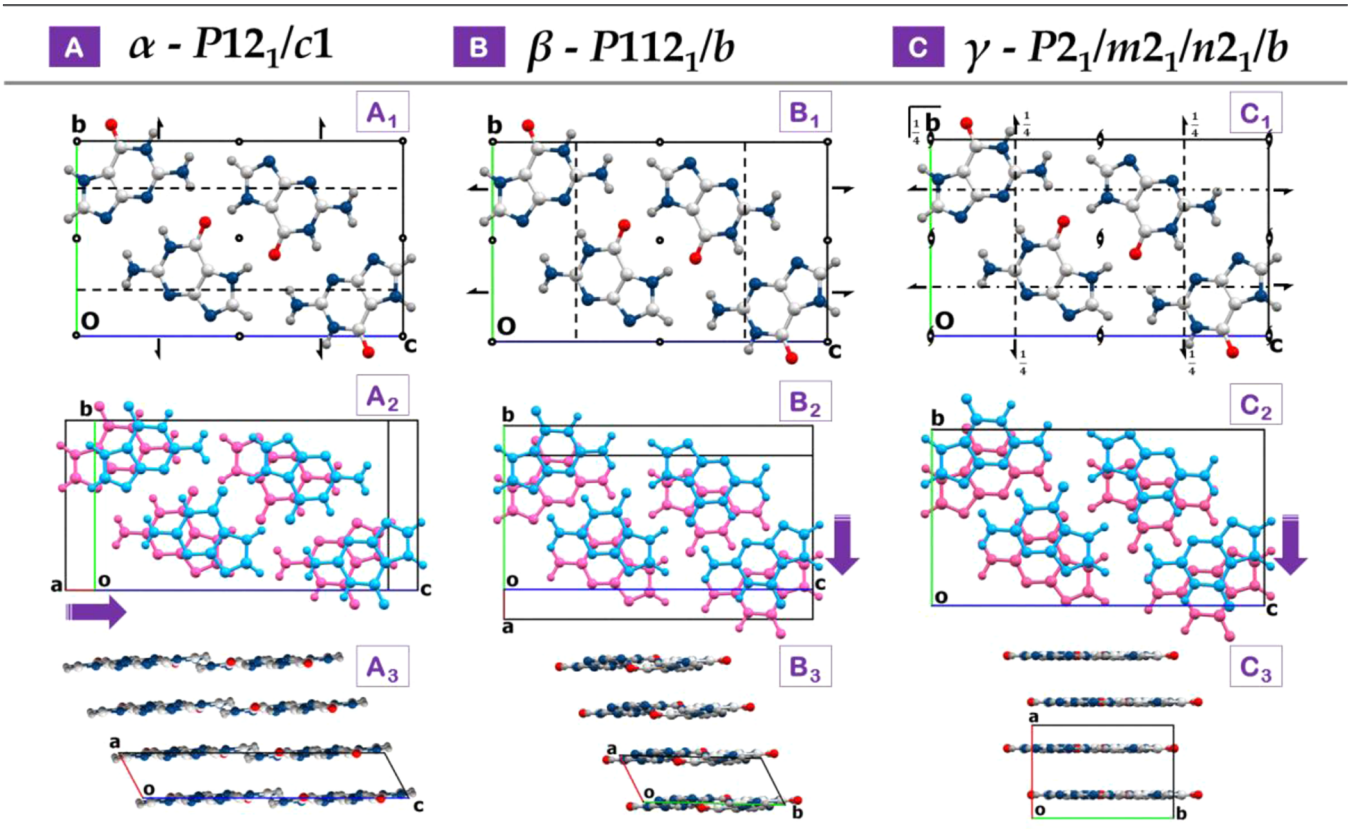

Figure 3. Three polymorphic (α, β, and γ) structures. (A) The monoclinic α-form. In panel A_1 the symmetry elements in the *bc* molecular layer are depicted, including the 2-fold screw axis (2_1) along the *b*-direction, the glide along the *c*-axis, and the center of inversion ($\bar{1}$). The translational offset of the H-bonded guanine layers along the *c*-axis is shown in (A_2). An edge-on view, along the *b*-axis, of the stacked molecular layers is shown in (A_3), exhibiting the "staircase" motif. (B) The same three different views of the monoclinic β-polymorph. Note that the direction of the 2_1-axis and the glide are interchanged with respect to the α-form (B_1). Moreover, the molecular layers are offset along the *b*-axis rather than the *c*-axis, as is evident in panels B_2 and B_3. (C) The same three views of the orthorhombic γ-polymorph. As for the symmetry elements depicted in (C_1), the molecules lie on a mirror (m) plane, and are related by *n*- and *b*-glide symmetry. The "translational" offset between neighboring molecular layers is along the *b*-axis as seen in panel C_2. An edge-on view along the *c*-axis, shown in C_3, displays the stacking arrangement of H-bonded molecules in the "zigzag" motif.

Å), to suggest the viability of the orthorhombic model.[36] We note, as an aside, that the $d(010)$ spacing of the monoclinic α-polymorph,[24] 9.69 Å, is close to that of the ED pattern of fish guanine (9.8 Å), but the $d(001)$ spacing in the monoclinic α-form (of 16.27 Å = 18.46 · sinβ) is inconsistent with the measured $d(001)$ spacing = 17.7 Å in the observed ED pattern, which would be required for the orthorhombic polymorph where β = 90°.

DOI: 10.1021/acs.chemmater.5b03549
Chem. Mater. 2015, 27, 8289−8297

We make use of the (0*kl*) ED pattern of fish guanine (Figure 1C) to guide us toward a hypothetical orthorhombic crystal structure. The only systematic absences in the ED pattern of fish guanine are for the 0*k*0 and 00*l* reflections. The implications of this constraint are that the hypothetical orthorhombic structure would not incorporate a glide plane perpendicular to the *a*-axis, where the glide direction would be along the *b*-axis, *c*-axis, or the *bc*-diagonal. Such a constraint eliminates several of the commonly observed space groups, leaving $P2_12_12_1$ and $P2_1/m2_1/n2_1/b$ (*Pmnb* in international short symbol, an alternative reoriented setting of the conventional *Pnma*) as the most likely orthorhombic candidates. The neighboring H-bonded *bc* layers in the hypothetical guanine structure of orthorhombic symmetry would be related by a 2_1-axis perpendicular to the layer. Given that the guanine molecules in the H-bonded layer form cyclic H-bonded dimers (Figure 2A) exhibiting pseudo 2/*m* symmetry, the neighboring layers would be related by pseudotranslation symmetry. With this structural information, we generated an ensemble of 45 structures, distinguished by successive 1 Å stepwise shifts along the *b* and *c*-directions, forming a two-dimensional grid of shifts across the 2_1 generated layer, which yielded all possible orthorhombic symmetries.

Of this ensemble of generated structures, only those with simulated 0*kl* electron diffraction patterns similar to that of the observed pattern were selected for further optimization based on DFT calculations. To our surprise, the structure found to have minimal energy (denoted above as the γ-form), which appeared in space group $P2_1/m2_1/n2_1/b$, exhibited an ED pattern very similar to the observed one, an issue elaborated below. Moreover, the pseudotranslational offset between neighboring molecular layers is very similar to that in the monoclinic β-polymorph. Thus, the crystal structures of the monoclinic β- and the orthorhombic γ-forms are very similar (Figure 3B_2,C_2). The main difference is that in the γ-form the layers are offset in a "zigzag" mode, while in the β-form the offset is of the "staircase" mode (Figure 3B_3,C_3), also exhibited by the α-form along a different axis (Figure 3A_3).

DFT OPTIMIZATION OF THE POLYMORPHIC STRUCTURES

Before calculating the optimized geometry of the newly proposed polymorphs, it is appropriate to validate the computational approach against the published α-form structure of the synthetic anhydrous guanine crystal.[24] The molecular layer motif, governed mainly by H-bonding, is reasonably well described by standard approximate exchange-correlation functionals for solid-state calculations, such as the generalized gradient approximation form due to Perdew, Burke, and Ernzerhof (PBE).[37] However, the stacking interactions are dominated by dispersion forces, for which the PBE functional is qualitatively inadequate and hardly predicts any binding.[33,38,39] This suggests that dispersive interactions must be included. Previous work on structural, electronic, and vibrational properties of monohydrate[40] and anhydrous[41] guanine also recognized the difficulty of treating dispersive interactions within standard exchange-correlation functionals. The problem was successfully circumvented by using the local density approximation (LDA), which mimics dispersive interactions through general overbinding. However, LDA performs poorly for hydrogen bonds.[42] Therefore, we chose instead to use the PBE functional, augmented by the pairwise dispersive corrections[33,38,39] of Tkatchenko and Scheffler (TS-vdW).[32] This approach yields quantitative accuracy for many different equilibrium and response properties of molecular solids with a variety of bonding scenarios.[33]

The agreement between the calculated and the experimental lattice parameters for the α-form, Figure 4, clearly demonstrates

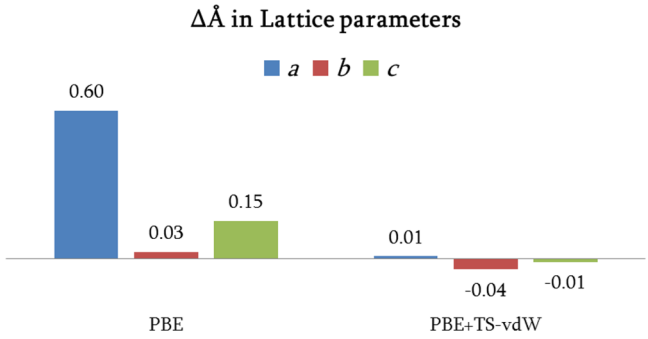

Figure 4. A plot of the differences (Å) between the lattice parameters of the computed and experimental[24] structures of the α-form. The calculated difference refers to structures computed using the PBE functional without and with dispersive corrections (TS-vdW). Absolute values of the lattice parameters are found in the Supporting Information (SI).

the success of the dispersion-corrected approach adopted here. Without corrections, the PBE-predicted *a* lattice parameter (along which dispersive interactions are most pronounced) overestimates experiment by 0.6 Å. Using the corrections, theory and experiment agreed within 0.01 Å along the same direction. A more modest but nonetheless meaningful improvement (from 0.15 to 0.01 Å) is obtained for the *c* lattice parameter, which is characterized by weaker H-bonds that have a significant dispersive content. At the same time, this did not come at the cost of accuracy in the *b* lattice parameter (from an overestimate of 0.03 Å to an underestimate of 0.04 Å), which is dominated by stronger H-bonds.

Following this validation, we proceeded to compute the optimized lattice parameters of the other two polymorphic structures, using the same dispersion corrected approach, and found them to be closely related to that of the original α-form (Table 1). The relative computed lattice energies of the α-, β-, and γ-polymorphs are 0, 0.4, and 1.0 kcal/mol (per molecule), respectively. This is at the limit of the expected accuracy of our computational approach.[33,42] Therefore, the α- and the β-forms could be considered as having similar lattice energies, with the γ-polymorph possibly also accessible.

POWDER LAB AND SYNCHROTRON X-RAY DIFFRACTION MEASUREMENTS

To experimentally establish which of the above-discussed polymorphs may correspond to the crystal structure of biogenic guanine, we performed X-ray powder diffraction using both synchrotron radiation and in-house measurements on various samples of synthetic and biogenic anhydrous guanine (Figure 5). As expected, the measured powder pattern of synthetic anhydrous guanine, obtained from DMSO solution, matches the published[24] simulated X-ray powder pattern of the α-polymorph (Figure 5A). In contradistinction, we obtained a synthetic β-polymorph following a procedure that involved crystallization of guanine from aqueous solution at pH 11 (Figure 5B). The interpretation of both diffractograms was validated by Rietveld refinement. The main difference between

DOI: 10.1021/acs.chemmater.5b03549
Chem. Mater. 2015, 27, 8289−8297

Table 1. Comparison of the Above-Defined α-, β-, and γ-Polymorphs of Anhydrous Guanine in Terms of Space Group Symmetry, Lattice Parameters (Å, deg, and Å^3), and Lattice Energy Differences (in kcal/mol, per molecule) Expressed Relative to That of the α-Polymorph[a]

	transformed α exptl[24]	calcd α-form	calcd β-form	calcd γ-form
space group	$P12_1/c1$	$P12_1/c1$	$P112_1/b$	$P2_1/m2_1/n2_1/b$
symmetry	monoclinic	monoclinic	monoclinic	orthorhombic
a	3.55	3.56	3.59	6.38
b	9.69	9.65	9.72	9.73
c	18.46	18.45	18.34	18.39
angle	118.3 (β)	118.5 (β)	119.5 (γ)	90
volume	560.1	557.9	557.6	1140.3
ΔE	–	**0 (ref)**	**0.39**	**0.96**

[a]All calculated results were obtained using the PBE+TS-vdW approach.

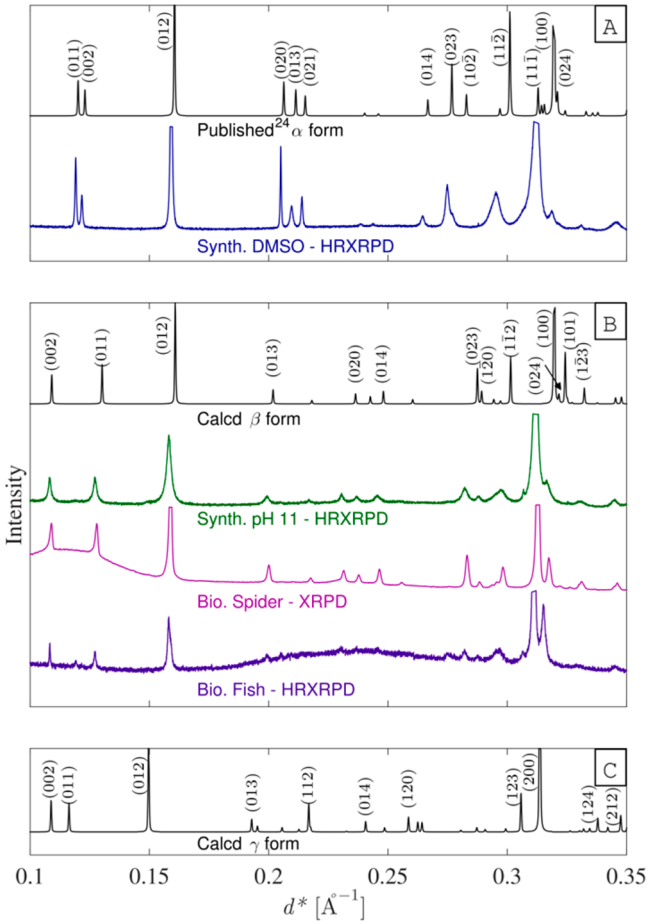

Figure 5. X-ray powder diffraction profiles. (A) Published[24] and synthetic α-form. (B) Calculated, synthetic, and biogenic β-form. (C) Calculated γ-form. To make all the reflections more visible, the intensity of the strongest reflection, such as (100), (200), and (012), were truncated. HRXRPD = high resolution powder X-ray diffraction.

the unit cell dimensions of the DFT-calculated and the Rietveld-refined experimental structures, for both polymorphs, is that the lattice parameters of the latter are slightly larger, by an average of ~0.6% (see SI for details). This difference is expected and attributed to thermal expansion, because the calculated structure was obtained at 0 K while the experimental diffractograms were collected at room temperature.

Further support for the different molecular stacking directions suggested in Figure 3 is obtained from a line profile analysis[43] (see Experimental and Computational Details). Comparison of the (002) and (020) reflections of the α- and β-forms revealed an opposite trend in the size of local d-spacing fluctuations, known as microstrain fluctuations (σ)[43] (Figure 6). The direction of increased fluctuations clearly correlates

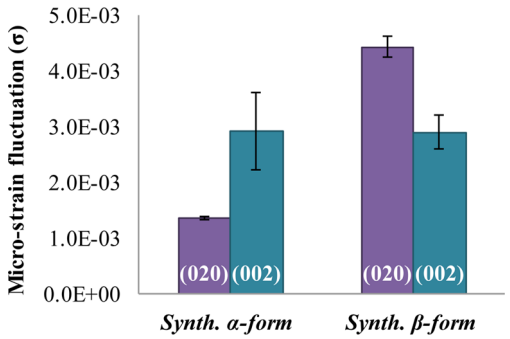

Figure 6. Microstrain fluctuation analysis for the synthetic α- and β-forms. The analysis compares the (020) and (002) reflections.

with the translational offset direction of the H-bonded layers, where variations are more likely. For the α-form, the translational offset is along the c-axis and the microstrain fluctuations are larger for the (002) reflection, whereas for the β-form the translational offset is along the b-axis and the microstrain fluctuations are larger for the (020) reflection.

The biggest surprise came upon re-examining the XRPD diffractogram of anhydrous guanine extracted from the white widow spider (*Latrodectus Pallidus*) reported by Levy-Lior et al.[8] We discovered an X-ray pattern identical to that of the calculated β-polymorph (Figure 5B). The sharp and distinct peaks displayed in the diffractogram reflect a crystallinity higher than that of guanine extracted from fish, consistent with the more isotropic cuboidal shape of the spider crystals. The elevated background for the d* values lower than 0.15 Å^{-1} is indicative of the presence of amorphous material in the sample and concurs with the suggestion of amorphous material-filled vesicles.[8]

The crystal structure of fish scale guanine also appears in the β-polymorph (Figure 5B). The fish scale guanine powder pattern is generally of lower quality than that of spider guanine (see ref 44). Nevertheless, there can be no question that the crystal structure has monoclinic symmetry, with the molecules arranged in the β-polymorph (Figure 3B).

Interestingly, the detailed Rietveld refinement analysis of X-ray reflections of fish scale guanine (Figure 7) reveals the presence of the α-form as a minor component. However, we are of the opinion that it does not originate from the biogenic

DOI: 10.1021/acs.chemmater.5b03549
Chem. Mater. 2015, 27, 8289−8297

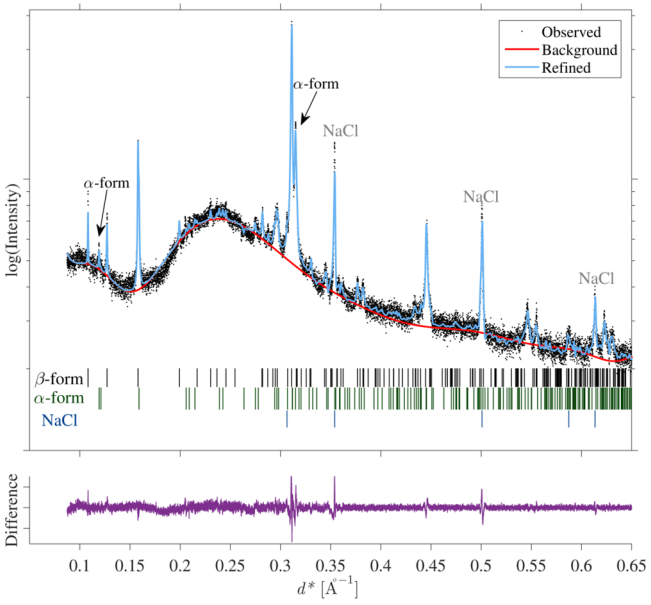

Figure 7. Rietveld refinement of HRXRPD diffractogram obtained from fish guanine. The calculated curve is obtained from three crystal structures: the β- and α-forms and NaCl. Despite the low quality of the diffractogram (see text for details), it is possible qualitatively to evaluate the relative content of the structures as 71%-β-form, 22%-α-form, and 7%-NaCl. The reflection positions of each structure are indicated by bars at the bottom of the figure, additional arrows indicating the position of the α-form, and the NaCl reflections. Full details of the refined results can be found in the SI, and also the Rietveld refinement of other samples: synthetic sample from DMSO, a sample synthesized using a solution at pH 11, and a sample of biogenic spider crystals.

crystallization process of fish guanine. Rather, as reported previously,[45] an amorphous guanine phase exists in the vicinity of the anhydrous guanine crystals that, once extracted from the cell environment and dried, may transform into the α-structure. The Rietveld refinement also revealed a minor contamination of NaCl.

Given the very small calculated difference in stability between the α- and β-forms, it would not be surprising to find that either may appear in the biogenic crystals. We also note that extreme nonphysiological conditions are used to obtain the α-form in vitro (organic solvents,[2] high temperature cycles[24]), suggesting that although possibly marginally more stable, the α-form may be kinetically less accessible. Under physiological conditions, so far only the β-form was observed, although this by no means serves as definite proof that the β-form is more stable in living organisms.

ELECTRON DIFFRACTION PATTERN OF FISH GUANINE

The measured high resolution XRPD (HRXRPD) patterns of biogenic guanine (Figure 5B and Figure 7) betray no hint of the presence of the proposed γ-polymorph, as evident from the absence of the (011) and (012) reflections of the γ-polymorph (Figure 5C) in the powder pattern. However, an excellent fit is found between the measured and the calculated (0kl) ED patterns of fish guanine, assuming its crystal structure adopts the γ-motif (Figure 8A). We are therefore faced with a conundrum: how can these two results be reconciled?

A clue to the answer is obtained by considering that the two diffraction methods complement each other; while the

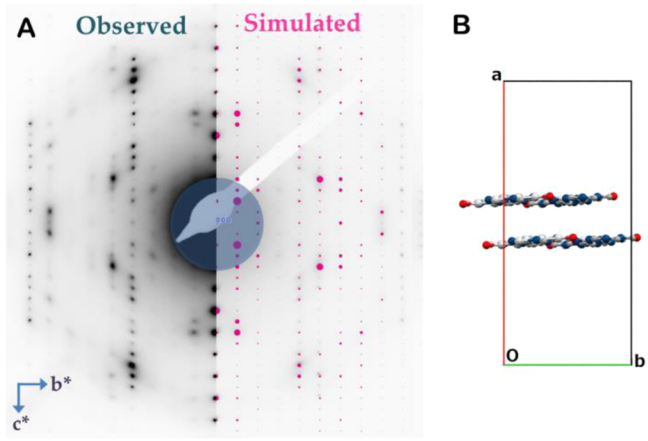

Figure 8. (A) The excellent agreement between the 0kl ED pattern obtained from fish guanine (left) and calculated for the γ-polymorph (right). (B) A highly similar ED pattern (see SI) is also obtained from the calculated structure shown in the figure, which comprises only two layers offset as in the β- or the γ-polymorph.

HRXRPD pattern is obtained from a large number of crystals in various orientations, the ED pattern is obtained from a single crystal of guanine. The method of electron diffraction allows the investigation of extremely small volumes because the amount of scattering is greater than for X-rays by a factor of 10^3 -10^4. However, the electron beam is attenuated much more rapidly, requiring very thin samples.[46] The guanine enigma may thus be resolved by assuming that the measured ED pattern arises from structural faults, which may be obtained in different ways, e.g., via a stacking fault composed of two H-bonded layers offset along the b-axis as in the β-motif, shown in Figure 8B; a fault composed of three such H-bonding layers yields an ED pattern which is already too dissimilar from that measured (see SI). Another possibility is a minor variant of the γ-motif (Figure 3C_3), composed of several layers, or a "twinning" mechanism in which the direction of the interlayer translational offset of a β-motif stack becomes reversed, yielding a structural fault. For all these different cases, the overriding mass of the crystal is arranged in the β-form, which should only contribute to the (00l) reflections in the ED pattern. To help rationalize the presence of the proposed structural faults, we note that the coherence length along the stacking a*-direction is about 35 $\pm$ 4 nm, which is by and large equal to the crystalline plate thickness (~30 $\pm$ 7 nm[25]) and therefore consistent with the presence of few structural faults, dispersed along the a*-direction in the β-form.

Finally, we note that the thin photonic plates of sapphirinidae copepods[9] are also made of anhydrous guanine, but the crystals are perfectly regular hexagons. In future work we will show, by use of electron diffraction, that the structure of copepod guanine is also of monoclinic β-symmetry and that the pseudohexagon morphology can be explained in terms of multiple crystal twinning.

CONCLUDING REMARKS

We have determined the structure of anhydrous guanine crystals obtained from fish and spider and have shown that it crystallizes in a monoclinic β-polymorph, which to the best of our knowledge has not been previously suggested. This β-form was generated by interchanging the 2-fold screw and glide symmetry elements of the α-form, resulting in a different offset

DOI: 10.1021/acs.chemmater.5b03549
Chem. Mater. 2015, 27, 8289−8297

between molecular layers. The lattice energies of these two polymorphs were found to be very similar, based on dispersion-corrected DFT calculations.

The β-polymorph yielded an excellent fit to the XRPD patterns of fish and spider guanine. However, the ED pattern of fish guanine, obtained with the plate-like crystal perpendicular to the electron beam, suggested an orthorhombic lattice. A generated orthorhombic γ-form with a structure akin to that of the monoclinic β-polymorph, but where the neighboring molecular layers are offset in a zigzag mode along the a-axis, yielded an ED pattern that matched the observed pattern almost perfectly. This created an enigma, resolved by assuming that the ED pattern arises from crystal structural faults composed of molecular layers offset as in the β- or γ-form. We suggest that this can be assessed further by using orientation-dependent ED measurements.

EXPERIMENTAL AND COMPUTATIONAL DETAILS

Materials. Biogenic crystals were extracted from the skin of the Japanese koi fish (*Cyprinus carpio*) using a method previously reported by Levy-Lior et al.[2] Synthetic crystals were recrystallized from anhydrous guanine, purchased from Sigma-Aldrich (lot SLBD6782 V). The α-form was recrystallized following a method previously reported by Levy-Lior et al.[2] The β-form was prepared by dissolving 0.1 g of guanine powder (Sigma–Aldrich) in 10 mL of 1 N NaOH (pH 14) inside a glass flask. HCl (1 N) was then titrated into the flask until the solution reached pH 11 and became cloudy due to the formation of small guanine crystals. The suspension was then filtered using a PVDF filter (0.22 mm) and dried overnight in a desiccator.

High-Resolution X-ray Powder Diffraction (HRXRPD). To study the crystal structure of guanine crystals experimentally, synchrotron HRXRPD was used to collect high quality diffractograms. Measurements were performed on ID22, the high-resolution powder diffraction beamline of the European Synchrotron Radiation Facility (ESRF, Grenoble, France), with λ = 0.39970(8) Å at ambient temperature. Instrument calibration was performed by using NIST silicon standards; final instrumental contribution to the full width at half-maximum (fwhm) did not exceed 2θ = 0.004.[47] The diffractograms were collected in the Debye–Scherrer geometry. The samples were inserted in a spinning 1 mm diameter borosilicate capillary, and the diffracted beam was monochromatized and collected by means of a multianalyzer stage equipped with a nine-point detector (for further information, http://www.esrf.eu/id22/technical-description). Nine diffractograms, obtained from each detector, were binned in a 2θ/intensity diffractogram. The measurements were performed on the synthetic α-form (obtained from DMSO), the synthetic β-form (obtained from NaOH:HCl at pH 11), and biogenic guanine obtained from koi fish.

Rietveld and Line Profile Analysis. To perform the Rietveld Analysis on the collected diffractogram, the GSAS-II software has been used.[48] Due to the well-known limit of powder diffraction in structural refinement of organic molecules, together with the limited crystal quality of the studied phases, a full refinement of the guanine intramolecular structure was not possible. A rigid-body refinement was performed instead. Using the GSAS-II RigidBody feature, the atoms of the guanine molecule were bonded together and the position and rotation angle and vector of the defined molecule were refined. Using this method, it was possible to reduce the refined parameters from 33 to 6 without losing the good description of the structure. Note that hydrogen atoms were not taken into consideration for the refinement because they are practically invisible to the X-ray diffraction. The transformed published structure[24] was used as an initial structure for the refinement of the α-form. For the β-form the calculated structure was used as an initial one. Peak intensities were determined by using Whole Profile Fitting.[49]

Negligible contribution of the diffractometer to the shapes of the diffraction lines allowed for the effective line profile analysis. Single diffraction peaks corresponding to a specific crystallographic plane were fitted to a Voigt function, which enabled independent evaluation of the contributions of the Lorentzian and Gaussian types corresponding to the coherence length (crystallite size) and microstrain fluctuations, respectively. Empirical formulas of high accuracy[50] are used to derive the average crystallite size and microstrain fluctuations. Profile fitting was performed using the Gnuplot 4.7 interface[51] over the most intense peaks of the diffractograms.

Electron Diffraction. Electron diffraction patterns were collected using a T-12 (Technical FEI) transmission electron microscope operated at 120 kV, using reported procedures.[2,8]

Density Functional Theory. The electronic structure, total energy, and geometry of the material structures were calculated by solving the Kohn–Sham equations of DFT within the generalized gradient approximation (GGA), using the PBE exchange-correlation functional.[37] The total energy was corrected by using Tkatchenko–Scheffler van der Waals (TS-vdW) pairwise dispersive corrections.[32] All calculations were carried out using the Vienna Ab Initio Simulation Package (VASP),[52] plane wave basis code, in which TS-vdW dispersive corrections were implemented.[53,54] The ionic cores were described by the projected augmented wave (PAW) method.[52,55] The planewave energy cutoff used for the calculations was 700 eV. For the monoclinic symmetry polymorphs (α and β), a 6 × 2 × 1 k-point grid sampling of the Brillouin zone was used, and for the orthorhombic symmetry polymorph (γ), a 3 × 2 × 1 grid was used. The k-points grids result in similar mesh density because in the orthorhombic polymorph the a-axis length is twice that of the monoclinic ones. The geometrical equilibrium structure, i.e., atomic positions and unit cell parameters, was obtained by using GADGET (see SI for details).[56] All forces in the system were relaxed to 10^{-4} eV/Å, and stress was relaxed to 10^{-2} kB.

Simulated Diffraction Patterns. The XRD diffractogram of the calculated polymorphs (α, β, and γ) were simulated using Materials Studio Reflex 6.1. The broadening of the XRD profile was performed following the Pseudo-Voigt model. The simulated ED patterns were obtained using the CrystalMaker-Single Crystal. The ED patterns shown in the article are "weighted reciprocal lattice" patterns, which combine intensity information (as calculated for electron diffaction) with the reciprocal lattice. The sizes of reciprocal lattice points are scaled in proportion to the corresponding intensity.

ASSOCIATED CONTENT

Supporting Information

The Supporting Information is available free of charge on the ACS Publications website at DOI: 10.1021/acs.chemmater.5b03549.

Structural details of the computed α-form. Rietveld refinement of the synthetic α-form sample (obtained from DMSO). Rietveld refinement of the synthetic β-form sample (obtained at pH 11), including a list of lattice parameters and atomic coordinates for the DFT-calculated β-form and Rietveld-refined structures. Rietveld refinement of the biogenic guanine of the spider crystals. Comparison of the simulated ED pattern of the γ-form and a supercell containing one, two, or three guanine H-bonded layers (PDF)

Structural file of the Rietveld refined β-form obtained synthetically (from pH 11) (CIF)

Structural file of the calculated β-form (CIF)

AUTHOR INFORMATION

Corresponding Authors

*E-mail: leeor.kronik@weizmann.ac.il.
*E-mail: lia.addadi@weizmann.ac.il.
*E-mail: leslie.leiserowitz@weizmann.ac.il.

Notes

The authors declare no competing financial interest.

DOI: 10.1021/acs.chemmater.5b03549
Chem. Mater. 2015, 27, 8289–8297

■ ACKNOWLEDGMENTS

We thank Prof. Stephen Weiner (Weizmann Institute) and Prof. Peter Rez (Arizona State University) for illuminating discussions, and Dr. Sharon Wolf for valuable assistance with electron diffraction measurements. This work has been supported by the Deutsch-Israelische Projektkooperation (DIP) program. B.P. acknowledges support from the European Research Council under the European Union's Seventh Framework Program (FP/2007−2013)/ERC Grant Agreement no. [336077].

■ REFERENCES

(1) Shawkey, M. D.; Morehouse, N. I.; Vukusic, P. A Protean Palette: Colour Materials and Mixing in Birds and Butterflies. *J. R. Soc., Interface* **2009**, *6*, S221−S231.
(2) Levy-Lior, A.; Pokroy, B.; Levavi-Sivan, B.; Leiserowitz, L.; Weiner, S.; Addadi, L. Biogenic Guanine Crystals from the Skin of Fish May Be Designed to Enhance Light Reflectance. *Cryst. Growth Des.* **2008**, *8*, 507−511.
(3) Land, M. F. The Physics and Biology of Animal Reflectors. *Prog. Biophys. Mol. Biol.* **1972**, *24*, 75−106.
(4) Gur, D.; Leshem, B.; Oron, D.; Weiner, S.; Addadi, L. The Structural Basis for Enhanced Silver Reflectance in Koi Fish Scale and Skin. *J. Am. Chem. Soc.* **2014**, *136*, 17236−17242.
(5) Rohrlich, S. T.; Rubin, R. W. Biochemical Characterization of Crystals from the Dermal Iridophores of a Chameleon Anolis Carolinensis. *J. Cell Biol.* **1975**, *66*, 635−645.
(6) Saenko, S. V.; Teyssier, J.; van der Marel, D.; Milinkovitch, M. C. Precise Colocalization of Interacting Structural and Pigmentary Elements Generates Extensive Color Pattern Variation in Phelsuma Lizards. *BMC Biol.* **2013**, *11*, 105.
(7) Teyssier, J.; Saenko, S. V.; van der Marel, D.; Milinkovitch, M. C. Photonic Crystals Cause Active Colour Change in Chameleons. *Nat. Commun.* **2015**, *6*, 6368.
(8) Levy-Lior, A.; Shimoni, E.; Schwartz, O.; Gavish-Regev, E.; Oron, D.; Oxford, G.; Weiner, S.; Addadi, L. Guanine-Based Biogenic Photonic-Crystal Arrays in Fish and Spiders. *Adv. Funct. Mater.* **2010**, *20*, 320−329.
(9) Gur, D.; Leshem, B.; Pierantoni, M.; Farstey, V.; Oron, D.; Weiner, S.; Addadi, L. Structural Basis for the Brilliant Colors of the Sapphirinid Copepods. *J. Am. Chem. Soc.* **2015**, *137*, 8408−8411.
(10) Doucet, S. M.; Meadows, M. G. Iridescence: A Functional Perspective. *J. R. Soc., Interface* **2009**, *6*, S115−S132.
(11) Oxford, G. S. Guanine as a Colorant in Spiders: Development, Genetics, Phylogenetics and Ecology. In *Proceedings of the 17th European Colloquium of Arachnology*, Edinburgh, 1997; Selden, P. A., Ed.; British Arachnological Society: Burnham Beeches, 1998, pp 121−131.
(12) Hinrichs, K.; Silaghi, S. D.; Cobet, C.; Esser, N.; Zahn, D. R. T. Ellipsometry from Infrared to Vacuum Ultraviolet: Structural Properties of Thin Anisotropic Guanine Films on Silicon. *Phys. Status Solidi B* **2005**, *242*, 2681−2687.
(13) Kinoshita, S.; Ghiradella, H.; Björn, L. O. Spectral Tuning in Biology II: Structural Color. In *Photobiology*; Björn, L. O., Ed.; Springer: New York, 2015; pp 119−137.
(14) Jordan, T. M.; Partridge, J. C.; Roberts, N. W. Non-Polarizing Broadband Multilayer Reflectors in Fish. *Nat. Photonics* **2012**, *6*, 759−763.
(15) Mueller, K. P.; Labhart, T. Polarizing Optics in a Spider Eye. *J. Comp. Physiol., A* **2010**, *196*, 335−348.
(16) Kreysing, M.; Pusch, R.; Haverkate, D.; Landsberger, M.; Engelmann, J.; Ruiter, J.; Mora-Ferrer, C.; Ulbricht, E.; Grosche, J.; Franze, K.; Streif, S.; Schumacher, S.; Makarov, F.; Kacza, J.; Guck, J.; Wolburg, H.; Bowmaker, J. K.; von der Emde, G.; Schuster, S.; Wagner, H. J.; Reichenbach, A.; Francke, M. Photonic Crystal Light Collectors in Fish Retina Improve Vision in Turbid Water. *Science* **2012**, *336*, 1700−1703.
(17) Zhao, Y.; Xie, Z.; Gu, H.; Zhu, C.; Gu, Z. Bio-Inspired Variable Structural Color Materials. *Chem. Soc. Rev.* **2012**, *41*, 3297−3317.
(18) Oaki, Y.; Kaneko, S.; Imai, H. Morphology and Orientation Control of Guanine Crystals: A Biogenic Architecture and Its Structure Mimetics. *J. Mater. Chem.* **2012**, *22*, 22686−22691.
(19) Iwasaka, M.; Miyashita, Y.; Mizukawa, Y.; Suzuki, K.; Toyota, T.; Sugawara, T. Biaxial Alignment Control of Guanine Crystals by Diamagnetic Orientation. *Appl. Phys. Express* **2013**, *6*, 037002.
(20) Mizukawa, Y.; Iwasaka, M. Magnetic Control of the Inclination of Biogenic Guanine Crystals Fixed on a Substrate. *J. Appl. Phys.* **2015**, *117*, 17B730.
(21) Setoguti, T. Ultrastructure of Guanophores. *J. Ultrastruct. Res.* **1967**, *18*, 324−332.
(22) Denton, E. J. Review Lecture: On the Organization of Reflecting Surfaces in Some Marine Animals. *Philos. Trans. R. Soc., B* **1970**, *258*, 285−313.
(23) Oxford, G. S.; Gillespie, R. G. Evolution and Ecology of Spider Coloration. *Annu. Rev. Entomol.* **1998**, *43*, 619−643.
(24) Guille, K.; Clegg, W. Anhydrous Guanine: A Synchrotron Study. *Acta Crystallogr., Sect. C: Cryst. Struct. Commun.* **2006**, *62*, o515−o517.
(25) Gur, D.; Leshem, B.; Oron, D.; Weiner, S.; Addadi, L. The Structural Basis for Enhanced Silver Reflectance in Koi Fish Scale and Skin. *J. Am. Chem. Soc.* **2014**, *136*, 17236−17242.
(26) The *mm* Laue symmetry implies that b^* is perpendicular to c^* and both lie in the plane corresponding to the plate face of the crystal. Furthermore, the a^* vector is perpendicular to b^* and c^* and is parallel to the zone axis.
(27) Leiserowitz, L.; Hagler, A. T. The Generation of Possible Crystal Structures of Primary Amides. *Proc. R. Soc. London, Ser. A* **1983**, *388*, 133−175.
(28) Gervais, C.; Coquerel, G. Simple Model Designed to Generate New Crystal Structures Derived from a Mother Phase; Application to Molecular Compounds. *Acta Crystallogr., Sect. B: Struct. Sci.* **2002**, *58*, 662−672.
(29) Pauchet, M.; Gervais, C.; Courvoisier, L.; Coquerel, G. Successful Application of the Derived Crystal Packing (DCP) Model in Resolving the Crystal Structure of a Metastable Polymorph of (±) Modafinil. *Cryst. Growth Des.* **2004**, *4*, 1143−1151.
(30) Pauchet, M.; Morelli, T.; Coste, S.; Malandain, J.-J.; Coquerel, G. Crystallization of (±)-Modafinil in Gel: Access to Form I, Form III, and Twins. *Cryst. Growth Des.* **2006**, *6*, 1881−1889.
(31) Price, S. L. Why Don't We Find More Polymorphs? *Acta Crystallogr., Sect. B: Struct. Sci., Cryst. Eng. Mater.* **2013**, *69*, 313−328.
(32) Tkatchenko, A.; Scheffler, M. Accurate Molecular Van Der Waals Interactions from Ground-State Electron Density and Free-Atom Reference Data. *Phys. Rev. Lett.* **2009**, *102*, 073005.
(33) Kronik, L.; Tkatchenko, A. Understanding Molecular Crystals with Dispersion-Inclusive Density Functional Theory: Pairwise Corrections and Beyond. *Acc. Chem. Res.* **2014**, *47*, 3208−3216.
(34) Rietveld, H. M. A Profile Refinement Method for Nuclear and Magnetic Structures. *J. Appl. Crystallogr.* **1969**, *2*, 65−71.
(35) Thewalt, U.; Bugg, C. E.; Marsh, R. E. The Crystal Structure of Guanine Monohydrate. *Acta Crystallogr., Sect. B: Struct. Crystallogr. Cryst. Chem.* **1971**, *27*, 2358−2363.
(36) On the assumption that the crystal structure is orthorhombic, the experimentally determined $d(010)$ and $d(001)$ spacings from the ED pattern are both lower by ∼4% than the length of the *b*- and *c*-axis, respectively, which may be due to an insufficiently accurate scaling constant. Multiplying the *d*-spacings by a factor of 1.04 yields values of 9.8 and 18.47 Å, respectively, which matches the H-bonding axial lengths very well.
(37) Perdew, J. P.; Burke, K.; Ernzerhof, M. Generalized Gradient Approximation Made Simple. *Phys. Rev. Lett.* **1996**, *77*, 3865−3868.
(38) Riley, K. E.; Pitoňák, M.; Jurečka, P.; Hobza, P. Stabilization and Structure Calculations for Noncovalent Interactions in Extended Molecular Systems Based on Wave Function and Density Functional Theories. *Chem. Rev.* **2010**, *110*, 5023−5063.

DOI: 10.1021/acs.chemmater.5b03549
Chem. Mater. 2015, 27, 8289−8297

(39) Klimeš, J.; Michaelides, A. Perspective: Advances and Challenges in Treating van Der Waals Dispersion Forces in Density Functional Theory. *J. Chem. Phys.* **2012**, *137*, 120901.
(40) Ortmann, F.; Hannewald, K.; Bechstedt, F. Guanine Crystals: A First Principles Study. *J. Phys. Chem. B* **2008**, *112*, 1540−1548.
(41) Lopes, R. P.; Marques, M. P. M.; Valero, R.; Tomkinson, J.; de Carvalho, L. A. Guanine: A Combined Study Using Vibrational Spectroscopy and Theoretical Methods. *Spectroscopy* **2012**, *27*, 273−292.
(42) Marom, N.; Tkatchenko, A.; Rossi, M.; Gobre, V. V.; Hod, O.; Scheffler, M.; Kronik, L. Dispersion Interactions with Density-Functional Theory: Benchmarking Semiempirical and Interatomic Pairwise Corrected Density Functionals. *J. Chem. Theory Comput.* **2011**, *7*, 3944−3951.
(43) Pokroy, B.; Fitch, A.; Zolotoyabko, E. The Microstructure of Biogenic Calcite: A View by High-Resolution Synchrotron Powder Diffraction. *Adv. Mater.* **2006**, *18*, 2363−2368.
(44) The poor crystallinity of the fish guanine diffractogram was mainly due to the morphology of the crystals and the limited amount of extractable material. In previous X-ray diffraction measurement by Levy-Lior et al.[2,8] only the stacking direction (100) was observed, due to strong preferred orientation caused by the anisotropic morphology of the platelet crystals. Yet, we were able to obtain more reflections, and thus determine the structure, although due to the low crystallinity some reflections are still missing. A possible reason for the relatively low quality of the HRXRPD pattern may be the extraction process of the crystals themselves from the fish scale, as well as some degree of impurity. It appears evident from the elevated background in the HRXRPD pattern at d^* values in the range 0.2−0.3 $Å^{-1}$ (Figure 7) that organic contamination, likely originating from cell debris, is present.
(45) Gur, D.; Politi, Y.; Sivan, B.; Fratzl, P.; Weiner, S.; Addadi, L. Guanine-Based Photonic Crystals in Fish Scales Form from an Amorphous Precursor. *Angew. Chem.* **2013**, *125*, 406−409.
(46) Hammond, C. *The Basics of Crystallography and Diffraction*; OUP: Oxford, 2009.
(47) Fitch, A. N. The High Resolution Powder Diffraction Beam Line at ESRF. *J. Res. Natl. Inst. Stand. Technol.* **2004**, *109*, 133−142.
(48) Toby, B. H.; Von Dreele, R. B. *GSAS-II*: The Genesis of a Modern Open-Source All Purpose Crystallography Software Package. *J. Appl. Crystallogr.* **2013**, *46*, 544−549.
(49) Pawley, G. S. Unit-Cell Refinement from Powder Diffraction Scans. *J. Appl. Crystallogr.* **1981**, *14*, 357−361.
(50) Pokroy, B.; Fitch, A. N.; Lee, P. L.; Quintana, J. P.; Caspi, E. N.; Zolotoyabko, E. Anisotropic Lattice Distortions in the Mollusk-Made Aragonite: A Widespread Phenomenon. *J. Struct. Biol.* **2006**, *153*, 145−150.
(51) Williams, T.; Colin K.. Gnuplot 4.7: An Interactive Plotting Program. http://www.gnuplot.info.
(52) Kresse, G.; Furthmüller, J. Efficient Iterative Schemes for Ab Initio Total-Energy Calculations Using a Plane-Wave Basis Set. *Phys. Rev. B* **1996**, *54*, 11169−11186.
(53) Al-Saidi, W. A.; Voora, V. K.; Jordan, K. D. An Assessment of the vdW-TS Method for Extended Systems. *J. Chem. Theory Comput.* **2012**, *8*, 1503−1513.
(54) Bučko, T.; Lebègue, S.; Hafner, J.; Ángyán, J. G. Tkatchenko-Scheffler van der Waals Correction Method with and without Self-Consistent Screening Applied to Solids. *Phys. Rev. B: Condens. Matter Mater. Phys.* **2013**, *87*, 064110.
(55) Kresse, G.; Joubert, D. From Ultrasoft Pseudopotentials to the Projector Augmented-Wave Method. *Phys. Rev. B: Condens. Matter Mater. Phys.* **1999**, *59*, 1758−1775.
(56) Bučko, T.; Hafner, J.; Ángyán, J. G. Geometry Optimization of Periodic Systems Using Internal Coordinates. *J. Chem. Phys.* **2005**, *122*, 124508.

DOI: 10.1021/acs.chemmater.5b03549
Chem. Mater. 2015, 27, 8289−8297